eXPRESS Polymer Letters Vol.11, No.9 (2017) 719–730
Available online at www.expresspolymlett.com
https://doi.org/10.3144/expresspolymlett.2017.69

Novel 3D porous semi-IPN hydrogel scaffolds of silk sericin and poly(*N*-hydroxyethyl acrylamide) for dermal reconstruction

S. Ross[1*], *M. Yooyod*[1], *N. Limpeanchob*[2], *S. Mahasaranon*[1], *N. Suphrom*[3], *G. M. Ross*[1]

[1]Biopolymer Group, Department of Chemistry, Biomaterials Excellent Centre, Faculty of Science, Naresuan University, 65000 Phitsanulok, Thailand
[2]Department of Pharmacy Practice, Faculty of Pharmaceutical Sciences, Naresuan University, 65000 Phitsanulok, Thailand
[3]Department of Chemistry, Faculty of Science, Naresuan University, 65000 Phitsanulok, Thailand

Received 20 January 2017; accepted in revised form 10 April 2017

Abstract. In this work, a novel semi-interpenetrating polymer network (semi-IPN) hydrogel scaffold based on silk sericin (SS) and poly(*N*-hydroxyethyl acrylamide) (PHEA) was successfully fabricated *via* conventional free-radical polymerization. The porous structure of the scaffolds was introduced using a lyophilization technique and the effect of cross-linker (XL) on morphology, gelation time and physical properties of hydrogel scaffold was first studied. The results show that using low cross-linker content (0.125, 0.25 and 0.5 wt% XL) produced flexible scaffolds and appropriate gelation times for fabricating the scaffold. Therefore, the polymerization system with a constant percentage of XL at 0.5 wt% was chosen to study further the effect of SS on the physical properties and cell culture of the scaffolds. It was observed that the hydrogel scaffold of PHEA without SS (PHEA/SS-0) had no cell proliferation, whereas hydrogel scaffolds with SS enhanced cell viability when compared to the positive control. The sample of PHEA/SS at 1.25 wt% of SS and 0.5 wt% of cross-linker was the most suitable for HFF-1 cells to migrate and cell proliferation due to possessing a connective porous structure, along with silk sericin. The results proved that this novel porous semi-IPN hydrogel has the potential to be used as dermal reconstruction scaffold.

Keywords: *polymer gels, biocompatible polymers, scaffolds, silk sericin, semi-IPN*

1. Introduction

Tissue engineering scaffolds have been extensively used in the field of biomedical applications during the last two-decades and continuously developed to overcome patient problems. Skin scaffolds are one of the most important biomaterials in the treatment of skin damage in particularly full-thickness wounds, in which the epidermis and all of the dermis is lost with a diameter of more than 4 cm [1–4]. Skin scaffolds incorporated with cultured cells which are subsequently placed on the skin can help patients endure less pain than conventional skin grafts. Generally, skin scaffolds are in three different fabricated forms; electrospinning fibers [5–11] porous materials [12, 13] and porous hydrogels [14], in which they can provide similar structure to the natural extracellular matrix (ECM). The materials used for fabrication into skin scaffolds are usually biocompatible, which benefits the use in the human body and they can be both natural polymers (i.e. chitosan [9, 12, 15, 16], cellulose acetate [17], collagen [18], gelatin [19–21] silk fibroin [5, 22], silk sericin [23]) and synthetic polymers (i.e. polylactide [9, 18], polyglycolide, poly (lactic acid)-co-glycolic acid [10, 24], polycaprolactone [11, 24, 25], polyethylene glycol [26], poly(vinyl alcohol) [6, 12, 27]). In terms of fabrication, both

*Corresponding author, e-mail: sukunyaj@nu.ac.th

natural and synthetic materials were notably blended together to enhance the mechanical properties of scaffolds for good cell support and attachment [5, 6, 8].
Silk fibers (from silk cocoons *Bombyx mori*) have received much attention in the field of natural materials, with applications such as skin tissue-engineering scaffolds. Silk fibers are composed of two layers; inside is a double strand of silk fibroin and outside this is silk sericin, which covers the silk fibroin. Both silk fibroin and silk sericin have shown benefits for use in medical applications, however, we decided to concentrate this work on silk sericin. Silk sericin is commonly ignored as a waste from the degumming process in silk industry, it generally has molecular mass greater than 200 kDa [28]. It is composed of 18 types of amino acids including up to 32% of the essential amino acids (serine, glycine, aspartic acid, glutamic acid, threonine and tyrosine) [29]. Sericin has bioactive properties, such as antioxidant, anti-elastase, anti-tyrosinase, anti-bacteria effect, moisturizing and mitogenic properties [29, 30]. It is also able to promote cell attachment, cell viability, cell proliferation and to modulate the release of bioactive molecules and drugs, or to impact the innate immune response of the host [30, 31].
Recently, silk sericin has seen an increase in its use in biomaterial scaffolds in conjunction with other biocompatible materials, such as collagen [32], gelatin [20, 23], hydroxyapatite [33] and poly(vinyl alcohol) [27], to overcome the mechanical and biological properties for promoting wound healing of scaffolds [29, 34–36]. However, there are only a few investigations on silk sericin with biocompatible materials for skin tissue regeneration. For example, silk sericin (SS) was fabricated together with poly(vinyl alcohol) (PVA) *via* freeze-drying and subsequent precipitated in various concentrations of ethanol [37]. When applying 70 vol% ethanol-precipitated PVA/SS scaffolds to the full-thickness wounds of rats, the wound size was reduced and showed higher extent of type III collagen formation and epithelialization, compared with the control scaffolds without sericin. Silk sericin was also covalent linked with collagen and hyaluronic acid in the presence of ethyl-3-(3-dimethylaminopropyl) carbodiimide and *N*-hydroxysuccinimide [38, 39]. When this scaffold had normal human dermal fibroblasts applied, the *in vitro* cell culture test indicated that this scaffold has a potential use in skin tissue engineering. In our previous work, we studied the conformational structure of silk sericin (*Bombyx mori*) stored at different temperatures and chose room-temperature silk sericin (RT-SS) to fabricate into 3D porous scaffold together with PVA, due to its mainly random coil conformational structure at this temperature [27].
A number of candidates containing hydroxyl polymer were selected to fabricate the scaffolds and from initial results *N*-hydroxyethyl acrylamide (HEA) was chosen. The acrylamide group presented in HEA allows for greater potential hydrogen bonding, while also giving a higher water content and flexibility to the system. In this work, therefore, RT-SS (called SS) was incorporated with HEA in the presence of *N*′*N*-methylene bisacrylamide (a cross-linker) *via* free-radical polymerization to form the semi-interpenetrating polymer network (semi-IPN) hydrogel scaffolds of PHEA/SS for the first time.
The reason to fabricate hydrogel scaffolds with the semi-IPN structure was because it provides a soft hydrogel scaffold with good mechanical properties and it can also swell in an aqueous solution like water but not in other solvents, similar to animal and human skin [40]. Semi-IPN hydrogels are composed of one cross-linked polymer network in the presence of another linear component that is not covalently bonded to the network. In addition, as sericin is not physically trapped into the gel but is present as an interpenetrate, the ability to hydrogen bond with the polymer network that introduces a hybrid system with the SS not fixed in the network but structurally flexible. The work started by studying the formulation of the polymerized semi-IPNs through the physical entrapment of SS within a cross-linked PHEA network. Then, the effect of cross-linker and silk sericin contents on the resultant PHEA/SS semi-IPN hydrogel scaffolds was observed in terms of gelation times, swelling ratio, morphology, *in vitro* degradation and cell proliferation of HFF-1.

2. Materials and methods

2.1. Materials

Silk cocoons (*Bombyx mori*) were obtained from Tak province in the North-East region of Thailand. Hydroxyethyl acrylamide (HEA), *N*′*N*-methylene bisacrylamide (*N*′*N*-MBAAm), ammonium persulfate (APS) and *N*,*N*,*N*′,*N*′-tetramethylethylenediamine (TEMED) were supplied by Sigma-Aldrich Co. Inc, Singapore. These chemicals were used to fabricate into the form of HEA hydrogels *via* free-radical polymerization. For cell culture test; feline fibroblast

cell line (HFF1) purchased from ATCC (American Type Culture Collection, USA), a medium of Dulbecco's modified eagle's medium (DMEM)/F12 and cell culture grade of dimethylsulfoxide (DMSO) were purchased from Sigma–Aldrich (St. Louis, MO, USA). Fetal bovine serum (FBS) and trypsin/EDTA (0.25%) were purchased from Gibco (Grand Island, NY). 3-(4,5-dimethlthiazol-2-yl)-2,5-diphenyltetrazolium bromide (MTT); ultra-pure grade was supplied by Amresco®, Solon, USA. Phosphate buffer saline (PBS) solution was prepared by dissolving 0.2 g NaCl, 1.16 g Na_2HPO_4, 0.2 g KH_2PO_4 and 0.2 g in 800 mL deionized water (DI water). The pH was adjusted to 7.4 with 1 M NaOH and then further DI water was added to make the solution to 1 L. The solution was dispensed into aliquots and sterilized by autoclaving before stored at 4 °C.

2.2. Method

2.2.1. Preparation of silk sericin powder

Silk sericin (SS) from silk cocoons was degummed using a hot water process, the same method used in our previous work [27]. The water degumming process was chosen, as it has no necessity to remove any chemicals normally used to extract SS, such as sodium carbonate, urea buffer, neutral soaps, or acidic solution by dialysis [41]. This is an environmental safe process and reduces the cost of fabrication. Briefly, the silk cocoons were cut into small pieces and boiled with purified water in the ratio of 20 g of silk cocoon pieces: 500 mL of water at 100 °C for 3 hours. After the degumming process, the SS solution was stored at room temperature and then dried for 24 hrs to achieve the silk sericin powders. In the water degumming process, approximately 20 wt% of silk sericin powder from 100 wt% of silk cocoons was achieved. The silk sericin powders were stored in a desiccator to protect from the moisture before

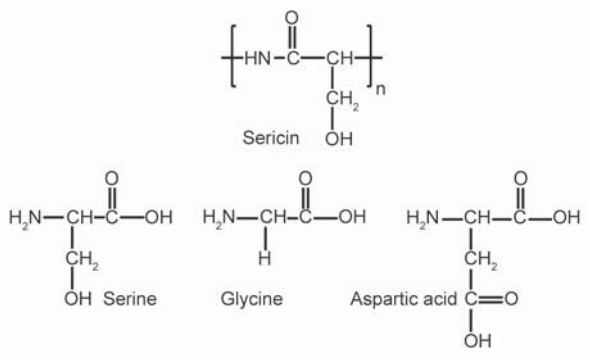

Figure 1. Chemical structure of sericin and its amino acids

further use. Figure 1 shows the chemical structure of sericin (represented by serine), and the most three abundant amino acids present in sericin (serine, glycine and aspartic acid).

2.2.2. Fabrication of semi-IPN hydrogel scaffolds

Semi-interpenetrating polymer networks (semi-IPN) composed of silk sericin (SS) and hydroxyethyl acrylamide (HEA) were prepared by conventional free-radical polymerization (see Figure 2). SS powders were first dissolved in hot water for 2 hrs and then HEA was added and continued to mix for 0.5 hr before adding *N*′*N*-MBAAm (cross-linker) and TEMED (catalyst) at 40 °C. This mixture solution was then left to room temperature before adding APS (initiator) to start the reaction and poured into 24 well-plates to form the semi-IPN hydrogels. As the polymerization is initiated by the redox pair of APS/TEMED, TEMED accelerates the rate of formation of free radicals from persulfate, which depends on the temperature used in the system in which the generated heat drives the reaction more quickly resulting in rapid polymerization. Therefore, room temperature (the most convenient for polymerization) was chosen to use for all samples.

After finishing the reaction, the semi-IPN hydrogel was washed by de-ionized water and ethanol several times to remove the unreacted monomers and chemicals before further use. Finally, the semi-IPN hydrogel was lyophilized to obtain a porous scaffold. The effect of the amount of cross-linker and SS onto the gelation time, release of silk sericin, swelling ratio, functional group, morphology and cell culture of scaffolds was studied. Table 1 shows the different samples used to prepare semi-IPN scaffolds. The 0.5% w/w of cross-linker was selected to study the effect of SS loading into the scaffolds.

2.2.3. Characterizations of semi-IPN hydrogel scaffolds of PHEA/SS

Gelation time

The polymerization times of each sample were recorded as gelation time. This gelation time was designated as the period of time required for gel formation after addition of the last component into the mixed solution (initiator). Therefore, gelation time was recorded from the initial time the initiator was added into the polymer solution until the formation of the gel structure (solid formation observed by naked eye). The experiments were repeated six times

Table 1. Formulations of semi-IPN porous hydrogel scaffolds of PHEA/SS *via* conventional free-radical polymerization

Sample code	HEA [g]	Sericin		Cross-linker [wt%]	TEMED [wt%]	APS [wt%]
		[g]	[wt%/v]			
Effect of cross-linker						
0% XL PHEA/SS-5	5.556	0.2500	5.00	–	0.50	0.50
0.125% XL PHEA/SS-5	5.556	0.2500	5.00	0.125	0.50	0.50
0.25% XL PHEA/SS-5	5.556	0.2500	5.00	0.250	0.50	0.50
0.5%XL PHEA/SS-5	5.556	0.2500	5.00	0.500	0.50	0.50
1%XL PHEA/SS-5	5.556	0.2500	5.00	1.000	0.50	0.50
2.0%XL PHEA/SS-5	5.556	0.2500	5.00	2.000	0.50	0.50
Effect of SS loading						
0.5%XL PHEA/SS-5	5.556	0.2500	5.00	0.500	0.50	0.50
0.5%XL PHEA/SS-2.5	5.556	0.1250	2.50	0.500	0.50	0.50
0.5%XL PHEA/SS-1.25	5.556	0.0625	1.25	0.500	0.50	0.50
0.5%XL PHEA/SS-0	5.556	–	–	0.500	0.50	0.50
0% XL PHEA/SS-0	5.556	–	–	–	0.50	0.50

under the same conditions and the average values were reported.

Swelling ratio

The swelling ratio was measured according to conventional gravimetric method. The semi-IPN porous hydrogel scaffolds of PHEA/SS (3 gels for each sample types) were immersed in deionized water at room temperature. The experiments were repeated three times under the same conditions and the average values were reported. The swelling ratio of the hydrogel scaffold was calculated as a ratio of wet weight and dry weight of hydrogel scaffold at time intervals, as shown in Equation (1):

$$\text{Swelling ratio} = \frac{W_t - W_0}{W_0} \tag{1}$$

where W_0 is the weight of the dried hydrogel scaffold and W_t is the weight of fully swollen hydrogel scaffold.

In vitro degradation

The *in vitro* degradation of the hydrogel scaffolds was studied by adding lyophilized hydrogel scaffolds into phosphate buffer saline (PBS, pH 7.4) at 37 °C and recording the percentage of weight loss during interval times using Equation (2);

$$\text{Weight loss}\,[\%] = \frac{W_d - W_f}{W_d} \cdot 100 \tag{2}$$

where W_d and W_f are the initial weight of lyophilized hydrogel scaffolds and the weight of lyophilized hydrogel after soaking in PBS solution and after dried, respectively. The experiments were repeated three times under the same conditions and the average values were reported.

Morphology

The morphology of semi-IPN porous hydrogel scaffolds (pore size, phase and interconnected structures) were monitored using a LEO model 1455VP scanning electron microscope (SEM). The lyophilized samples were cryo-fractured in liquid nitrogen to give cross-sectioned samples and then mounted on metal stubs and coated with gold to give higher electron density covered before testing.

In vitro cell culture test

Preparation of cell lines

Feline fibroblast cell lines (HFF1) were maintained in a 75 cm^2 culture flask at 37 °C under 5% CO_2 humidified atmosphere. The cells were grown in DMEM/F12 medium supplemented with 10% FBS. The culture medium was replaced every 2 days.

Fibroblast seeding and culture on hydrogel scaffolds

Hydrogel scaffolds were cut into cubes (0.3 cm^3) and immersed in 70% ethanol for 0.5 hr followed by washing with phosphate buffer saline (PBS, pH 7.4) several times before further use. Then, the sterilized scaffolds were immersed in 1 mL of the medium (90 DMEM:10 FBS) and left for overnight in incubator at 37 °C and dehydrated in a cell culture hood for 3 hours to achieve partially dehydrated scaffolds. Feline fibroblast cell line (HFF1) ($1 \cdot 10^6$ cells) with 200 μL medium was dropped slowly on the top of the partially dehydrated scaffolds. They were seeded into 24 well-plates and allowed cells to attach for 24 hrs

before adding another 1 mL of medium. Scaffolds with loaded cells were incubated for 2 days at 37 °C, the medium was changed and left for another day before doing the MTT assay [27].

Cell proliferation: MTT assay

The cell proliferation of the fabricated hydrogel scaffolds was investigated by MTT assay. On days 3, 7 and 14, the exhausted media of the cell with hydrogel scaffolds were replaced with MTT solution and incubated for 4 hrs at an incubated temperature of 37 °C with 5% CO_2. The formazan crystals were dissolved in DMSO and the optical density (OD) was measured at the wavelength of 490 nm using a spectrophotometric microplate reader, the absorbance corresponded to the number of cell proliferation [40]. All experiments were performed in triplicate. In this method, the active mitochondria of the viable cells reduce the yellow colored solution of MTT (3-(4, 5-dimethylthiazol-2-yl)-2, 5-diphenyltetrazolium bromide, a yellow tetrazole) into blue colored formazan crystals, which corresponds to cellular viability.

3. Results and discussion

3.1. Fabrication of semi-IPN hydrogel scaffold of PHEA/SS

The porous semi-IPN hydrogel scaffolds of poly(hydroxyethyl acrylamide) (PHEA) and silk sericin (SS) was successfully prepared by a conventional radical polymerization of hydroxyethyl acrylamide in the presence of SS for the first time. SS used in this work is the silk sericin prepared from a hot water degumming process and stored at room temperature before converting into powder, following the same method as our previous work, which studied the conformational structure of silk sericin [27]. The conformational structure of silk sericin used in this work is mostly random coils that allows silk sericin to be dissolved in hot water more easily and therefore, suitable to be incorporate in a water-based polymerization system.

Two sets of experiments investigating the preparation of semi-IPN scaffolds were studied. The first experiment examined the effect of the concentration of cross-linker and the second studied the effect of silk sericin content onto the properties of scaffolds, as seen in Table 1. A pure PHEA sample was also fabricated through free radical polymerization and used as the controlled sample and named 0% XL PHEA/SS-0. The semi-IPN was formed in which the SS chains were entrapped in the polymer networks of PHEA. Figure 2 shows the schematic illustration of this conventional polymerization together with a drawing of semi-IPN networks of PHEA/SS.

After fabrication of the hydrogel scaffolds the next step was the lyophilization of the hydrogels to

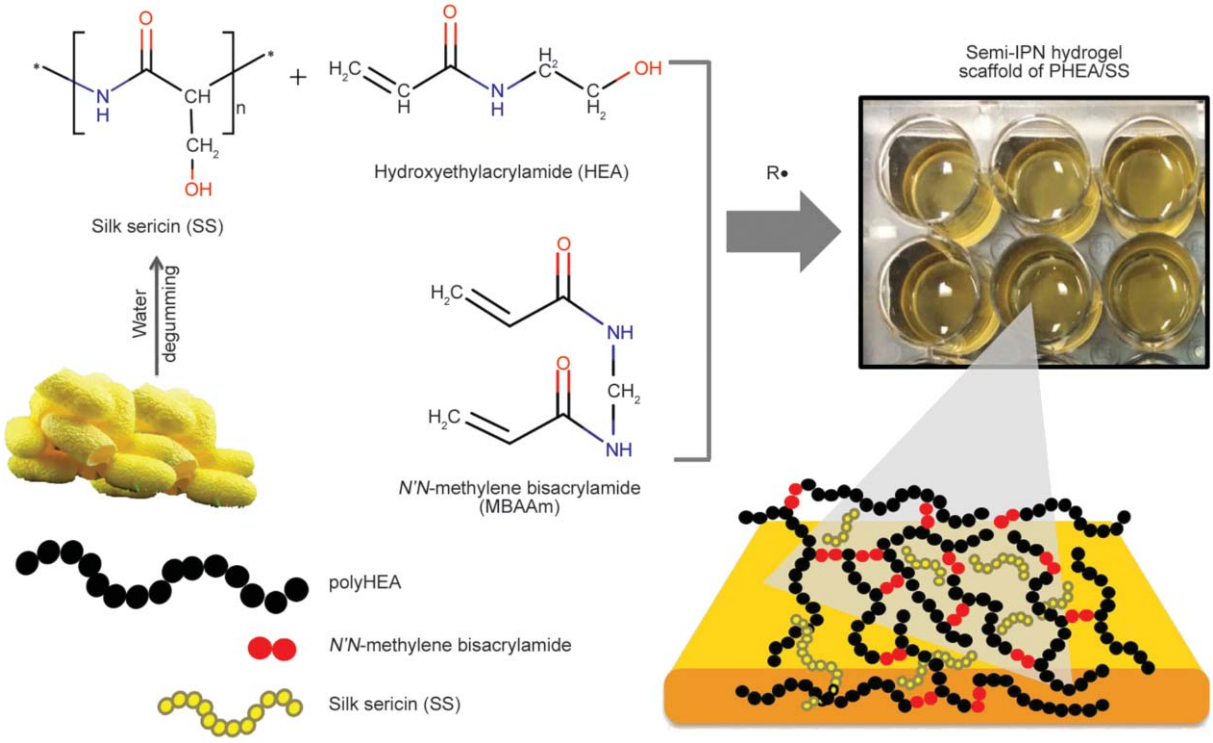

Figure 2. Schematic picture of synthetic semi-IPN hydrogel scaffold of PHEA/SS *via* conventional free-radical polymerization

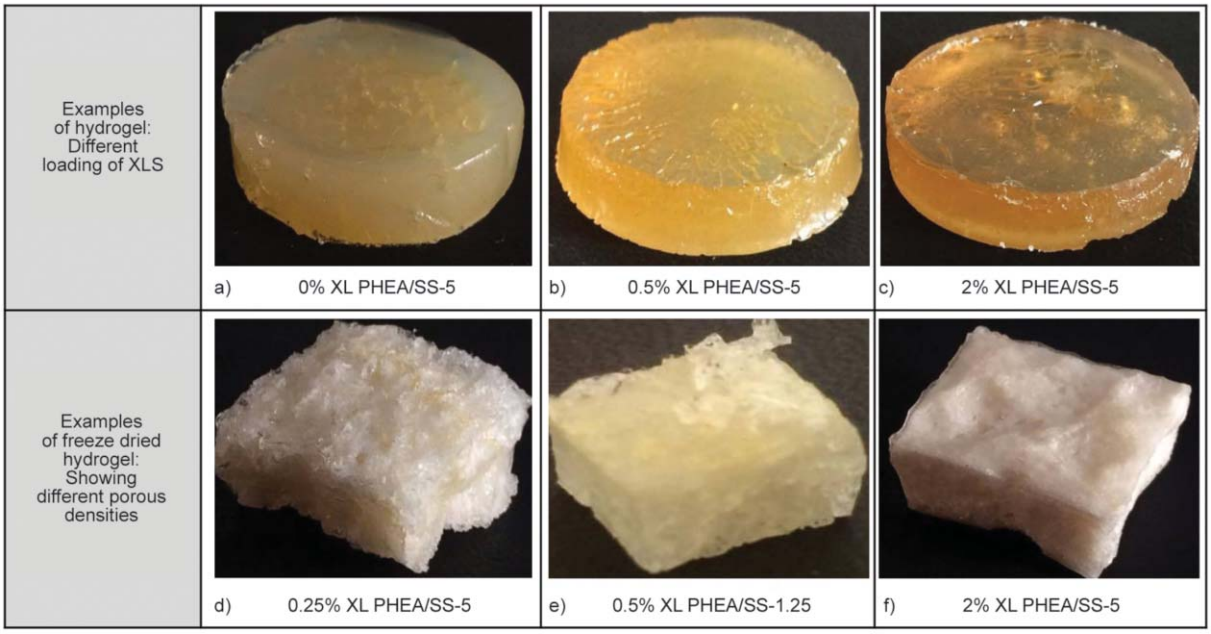

Figure 3. Physical appearance of semi-IPN hydrogel scaffolds before (a, b and c) and after lyophilization (d, e and f)

promote a porous structure. Figure 3 shows the physical appearances of examples of semi-IPN hydrogel scaffold of PHEA/SS before and after lyophilization. The polymerized hydrogels at the same loading of silk sericin (5 wt%) with different concentrations of cross-linkers showed differences in clarity in which higher loading of cross-linker produced a more transparent and harder hydrogel than lower loading of cross-linker. Surprisingly, the PHEA/SS without cross-linker (Figure 3a) was able to form a very soft viscous 'gel'. This is possible mainly due to the physical bonding between the –NH and –OH groups containing in PHEA and SS molecules. After lyophilization, porous structures were seen in all hydrogels of PHEA/SS but with different densities depending on the loading of cross-linker and SS. At the same loading of SS (Figure 3d and 3f) but different concentration of cross-linker, low cross-linker content had higher density of porous structures and higher amounts of cross-linker produced harder hydrogels. Figure 3e shows the lyophilized scaffold that has physical properties in between Figure 3d and 3f.

3.2. Effect of cross-linker loading to semi-IPN hydrogel scaffold of PHEA/SS

The different loading of cross-linker (XL) from 0 to 2.0% wt of total weight of HEA and SS was used to prepare semi-IPN hydrogels of PHEA/SS. The amount of SS was controlled at 5 wt% of all samples. As discussed earlier, the percentage of cross-linker impacted the physical properties of hydrogel, high cross-link concentration promoted hardness in the hydrogel as well as a less porous structure. It also effected the gelation time of the hydrogels, timed from the addition of APS to complete gelation. The gelation times of each sample were observed and shown in Figure 4. The fastest gelation was 1.25 mins when using high loading of cross-linker at 2.0 wt% and the results show that the gels contain 0–0.5% XL took approximately 1 min longer. However, using cross-linker at 0, 0.125, 0.25 and 0.5 wt% showed only a small change in gelation time. Whereas, higher amount of cross-linker altered the polymerization times of these semi-IPN hydrogels. The study of the gelation time is important for controlling the properties of hydrogels

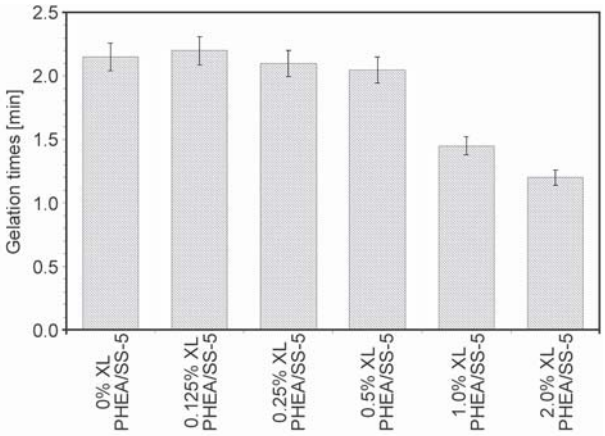

Figure 4. Gelation times of semi-IPN hydrogel scaffold of PHEA/SS with different loadings of cross-linker. Data points of the figure present the mean ±SD (n = 6).

and especially it is important key factor in terms of fabrication on larger scales.

The morphology of all lyophilized hydrogel scaffolds, which were cryo-fractured in liquid nitrogen, were also investigated by SEM and the results are presented in Figure 5. All these hydrogel scaffolds had porous structures with different sized diameters and distribution, in which hydrogel scaffold of PHEA/SS without cross-linker showed the biggest porous diameter size of approximately 100 μm (Figure 5a). Using more cross-linker to create the polymer networks of PHEA caused smaller pore size diameter in these semi-IPN hydrogel scaffolds, which is in ranges of 10–50 μm. The smallest number of pores was observed in the composition that used 2 wt% of cross-linker (Figure 5f) due to the high crosslink density in this hydrogel structure.

The swelling ratios of these PHEA/SS semi-IPN hydrogel scaffolds were also investigated. This value described the capability of the hydrogel scaffolds to accumulate water into their polymer networks during the time of immerging into the water compared to

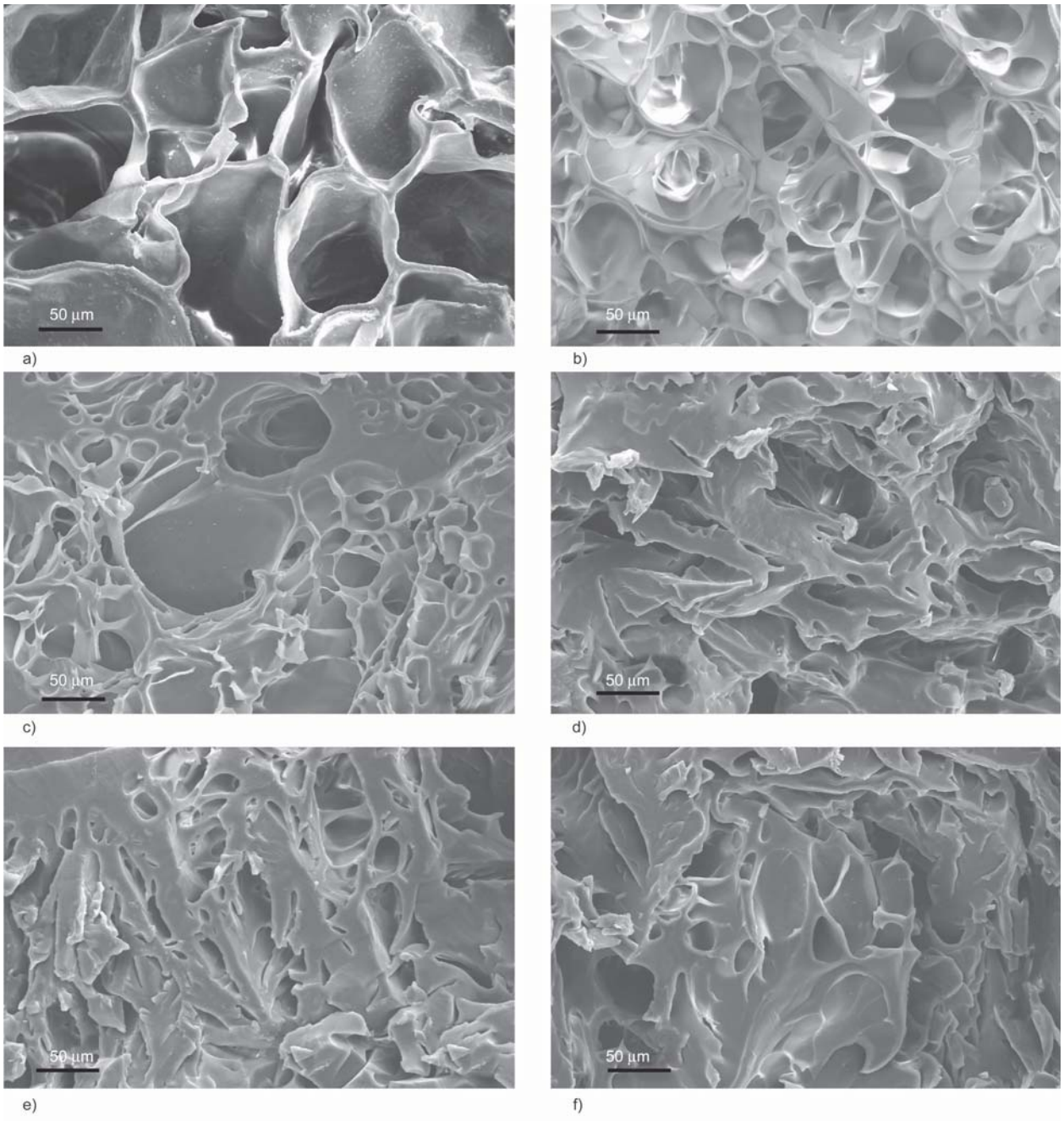

Figure 5. SEM images of lyophilized semi-IPN hydrogels scaffold of PHEA/SS at 5 wt% of SS and different loading of cross-linker: a) 0% XL PHEA/SS-5, b) 0.125% XL PHEA/SS-5, c) 0.25% XL PHEA/SS-5, d) 0.5% XL PHEA/SS-5, e) 1.0% XL PHEA/SS-5 and f) 2% XL PHEA/SS-5

the dried hydrogel scaffold. The results from Figure 6 show that the hydrogel scaffold without cross-linker of 0% XL PHEA/SS-0 and 0% XL PHEA/SS-5 showed significantly higher swelling ratios than that of hydrogel scaffolds with using cross-linker due to no chemically cross-linked network in its structure. However, adding SS into this hydrogel reduced the swelling properties of the gel, this is due to more hydrogen bonding of SS and PHEA, which lowers the bonding sites available to entrap water molecules in the cross-linked hydrogel network. Using higher percentage of cross-linker (0.125, 0.25 and 0.5% XL) showed similar value of swelling ratio, whereas 2% XL PHEA/SS-5 had lowest swelling ratio due to having the highest cross-linked density in its structure. This result corresponds to the results from SEM images, as higher cross-linked density in the hydrogel scaffolds the lower number of porous structures were produced and then caused to the lower swelling ratio.

In summary, it was found that the cross-linker loading effected the gelation time, morphology and swelling ratio of semi-IPN hydrogel scaffold of PHEA/SS at the controlled amount of SS (5 wt%). The hydrogel scaffold without cross-linker showed significant differences in its physical properties and morphology from hydrogel scaffolds with cross-linker. In addition, we observed that SS helps to improve the flexibility of the hydrogel scaffolds, as compared to the PHEA sample (no SS added). Based on physical properties of hydrogels using concentration of cross-linker at 0.5 wt%, which is flexible and shows good distribution of porous structure (better than 0.125 and 0.25 wt%) with a porous size in range of 10–50 μm, it was chosen to study further the effect of SS loading onto the hydrogel scaffolds by controlling the percentage of cross-linker at 0.5 wt% in the next experiment.

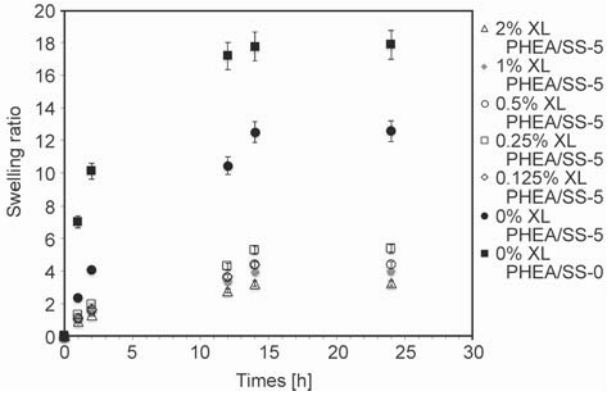

Figure 6. Swelling ratio of porous semi-IPN hydrogels scaffold of PHEA/SS at 5 wt% of SS and different loading of cross-linker. Data points of the figure present the mean ±SD (n = 3).

3.3. Effect of silk sericin loading to semi-IPN hydrogel scaffold of PHEA/SS

Four different concentrations of silk sericin (SS) (0, 1.25, 2.5 and 5 wt%) were added during the polymerization of hydrogels at the constant amount of 0.5 wt% cross-linker. The gelation time of these PHEA/SS semi-IPN hydrogel was investigated and shown in Figure 7. In addition, a sample of PHEA without either cross-linker and SS was also prepared (0% XL PHEA/SS-0) and presented the longest gelation time. This hydrogel was very soft and less coherent when compared to the other hydrogels containing cross-linker due to having only physical interactions between polymer chains (no covalent bonds). The hydrogel scaffold without SS (0.5% XL PHEA/SS-0) had the shortest time to polymerize when compared with the other hydrogels. Increasing SS loading resulted in longer gelation times. In this case, longer gelation times are obtained because higher amount of silk sericin chains obstructs the growth of PHEA chains and the network structure. Also, high amounts of SS, effectively dilutes the concentration of monomer and initiator.

The SEM images of the cross-sectioned PHEA/SS hydrogel scaffolds with different loadings of SS at the control cross-linker content (0.5 wt%) were also observed by fracturing the lyophilized scaffolds in liquid nitrogen (results presented in Figure 8). The hydrogel scaffold without SS (Figure 8a) showed the

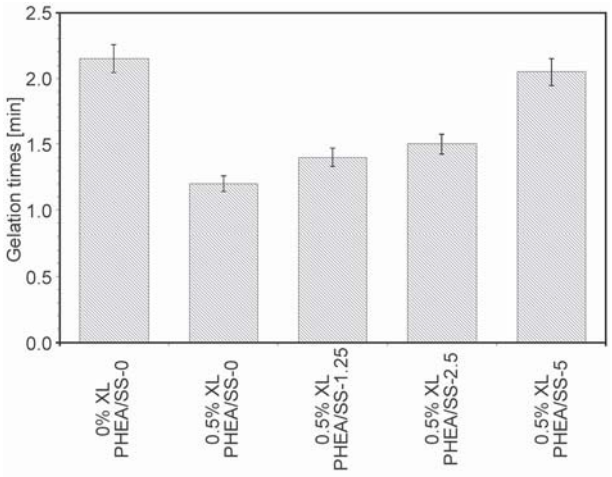

Figure 7. Gelation times of semi-IPN hydrogel scaffold of PHEA/SS with different sericin loading at 0.5 wt% of cross-linker. Data points of the figure present the mean ±SD (n = 6).

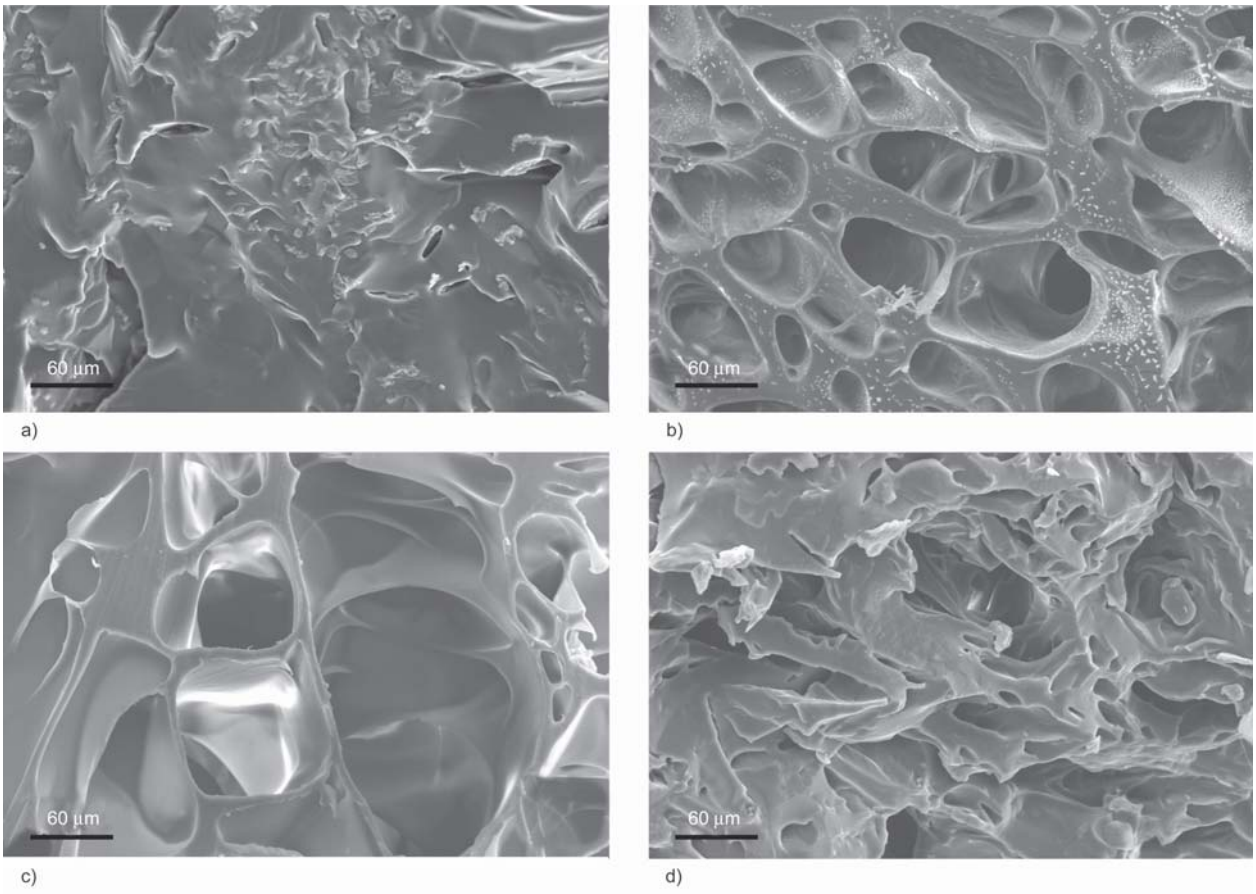

Figure 8. Images of semi-IPN hydrogel scaffold of PHEA/SS with different sericin contents at 0.5 wt% of cross-linker; a) 0.5% XL PHEA/SS-0; b) 0.5% XL PHEA/SS-1.25; c) 0.5% XL PHEA/SS-2.5 and d) 0.5% XL PHEA/SS-5

smallest number of pores compared to hydrogels with SS (Figure 8b, 8c, and 8d). Between the scaffolds with added SS, differences in pore size diameter and uniformity of the structures were observed in ranges of 10–100 µm. The hydrogel sample of 0.5% XL PHEA/SS-1.25 (Figure 8b) shows the most regularity in interconnecting porous structures and has a diameter size range of 30–100 µm.

Beside of the study of morphology of the samples, several other characterization techniques were used; these included; swelling ratio, release of SS, *in vitro* degradation and the cell culture test. This was in order to observe and find the best composition suitable for both polymerization into a semi-IPN hydrogel scaffold and for use in skin reconstruction applications.

Figure 9 shows the swelling ratio of PHEA/SS semi-IPN hydrogel scaffold with different sericin contents at 0.5 wt% of cross-linker. The sample with no cross-linker and SS shows the highest swelling ratio and is significantly different from other the samples that contain 0.5% XL. The cross-linked hydrogel without SS (0.5% XL PHEA/SS-0) shows higher swelling ratio than that of hydrogels with added SS. However, there is no difference in the swelling behavior between SS contents of 1.25, 2.5 and 5 wt%. This indicates that cross-linking the network has the largest effect on the swelling behavior of the hydrogels and the addition of SS as an interpenetrate produced an effect but this effect was similar at all tested concentrations (1.25–5 wt%).

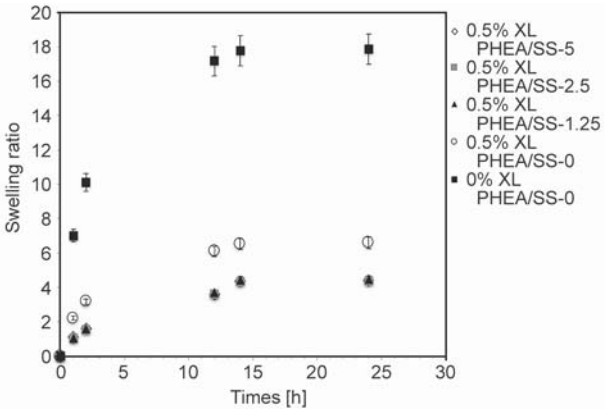

Figure 9. Swelling ratio of porous semi-IPN hydrogels scaffold of PHEA/SS at 0.5 wt% of cross-linker and different loading of SS. Data points of the figure present the mean ±SD (n = 3).

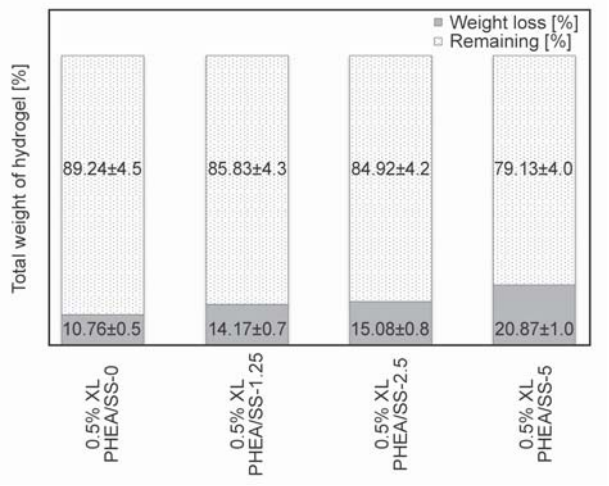

Figure 10. *In vitro* degradation of semi-IPN hydrogel scaffold of PHEA/SS with different sericin contents at 0.5 wt% of cross-linker. Data points of the figure present the mean ±SD (n = 3).

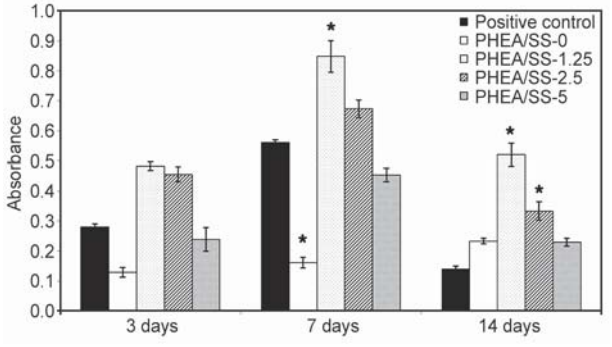

Figure 11. Cell proliferation of HFF-1 on semi-IPN hydrogel scaffolds of PHEA/SS with different sericin contents at 0.5 wt% of cross-linker, and positive control (polystyrene plates) after 3, 7 and 14 days of culture. Data points of the figure present the mean ±SD (n = 3), analyzed statistically using One-way ANOVA-test and Bonferroni Post-hoc test (*p < 0.05).

The *in vitro* degradation for 30 days was observed and shows the amount of sericin (SS) released from the PHEA/SS semi-IPN hydrogel scaffolds depended on the sericin content. Increasing sericin content (increases hydrophilic content) shows greater sericin release (Figure 10), which can cause breaks in the hydrogel network resulting in greater degradation. The *in vitro* degradation of hydrogel scaffolds without SS was also observed and showed lowest % weight loss due to having no sericin available to be released.

This work also studied the cell proliferation of HFF-1 on the PHEA/SS semi-IPN hydrogel scaffolds with different sericin contents at 0.5 wt% of cross-linker, and a positive control (polystyrene plates) after 3, 7 and 14 days of culture, the results are presented in Figure 11.

The results for the positive control shows its highest cell viability at days 3 and day 7 and then decreases at day 14. This is due to the high growth rate of fibroblast cell competing for space until there is not enough space for cell growth, which causes the cells to die. The hydrogel scaffold of PHEA without SS (PHEA/SS-0) had no cell proliferation, whereas hydrogel scaffolds with SS supported cell viability when compared to the positive control. This confirms that using SS promotes cell viability in these semi-IPN hydrogel scaffolds. All semi-IPN hydrogel scaffolds of 1.25, 2.5 and 5 wt% of SS show the highest cell proliferations at day 7 and then a decrease is seen at day 14 because high cell growth causes a reduced in space for cell to adhere and finally some cells die similar to the positive control. Comparing day 3 and 7 of culture, it can be seen that the hydrogel scaffolds of PHEA/SS-1.25 showed higher cell proliferation than both PHEA/SS-2.5 and PHEA/SS-5. The decrease in cell proliferation when using high SS contents maybe due to more SS being released into culture medium, (as confirmed by sericin release result). It has been reported previously that free SS may have some cytotoxic effect on cells [42]. Therefore, the semi-IPN hydrogel scaffold of PHEA/SS-1.25 is the most suitable for fibroblast cell to migrate easily and then promote cell proliferation due to having the connective porous structure with an ideal pore size diameter of 30–100 μm and especially containing of appropriate loading of silk sericin.

4. Conclusions

A novel semi-IPN porous hydrogel scaffold of PHEA/SS was successfully fabricated *via* conventional free-radical polymerization for potential use as a dermal reconstruction material. The characteristic properties of scaffolds; porous size, structure and arrangement, gelation time and swelling ratio, were dependent on the amount of cross-linker and concentration of silk sericin used in the system. The semi-IPN porous hydrogel scaffold of PHEA/SS at 1.25 wt% of silk sericin and 0.5 wt% of cross-linker loadings was the most suitable for fibroblast cells allowing easy migration and then promotion of cell proliferation due to having a connective porous structure along with containing silk sericin. In addition, it was observed that adding silk sericin in ranges of 1.25–5.0 wt% into the hydrogel scaffolds containing 0.5 wt% cross-linker gave good compatibility with the HFF1 fibroblast cell line and promoted cell

proliferation and cell adhesion as well as helps to improve the flexibility of the hydrogel scaffolds.

Acknowledgements

The authors are thankful to National Research Council of Thailand 2014 (research number 93266) for funding this project and Science Lab Centre, Faculty of Science, Naresuan University for supporting the measurements.

References

[1] Yildirimer L., Thanh N. T. K., Seifalian A. M.: Skin regeneration scaffolds: A multimodal bottom-up approach. Trends in Biotechnology, **30**, 638–648 (2012). https://doi.org/10.1016/j.tibtech.2012.08.004

[2] MacNeil S.: Biomaterials for tissue engineering of skin. MaterialsToday, **11**, 26–35 (2008). https://doi.org/10.1016/S1369-7021(08)70087-7

[3] Herndon D. N., Barrow R. E., Rutan R. L., Rutan T. C., Desai M. H., Abston S.: A comparison of conservative versus early excision. Therapies in severely burned patients. Annals of Surgery, **209**, 547–552 (1989).

[4] Herndon D. N., Parks D. H.: Comparison of serial debridement and autografting and early massive excision with cadaver skin overlay in the treatment of large burns in children. Journal of Trauma-Injury Infection and Critical Care, **26**, 149–152 (1986). https://doi.org/10.1097/00005373-198602000-00009

[5] Sill T. J., von Recum H. A.: Electrospinning: Applications in drug delivery and tissue engineering. Biomaterials, **29**, 1989–2006 (2008). https://doi.org/10.1016/j.biomaterials.2008.01.011

[6] Agarwal S., Wendorff J. H., Greiner A.: Use of electrospinning technique for biomedical applications. Polymer, **49**, 5603–5621 (2008). https://doi.org/10.1016/j.polymer.2008.09.014

[7] Ramakrishna S., Fujihara K., Teo W-E., Yong T., Ma Z., Ramaseshan R.: Electrospun nanofibers: Solving global issues. MaterialsToday, **9**, 40–50 (2006). https://doi.org/10.1016/S1369-7021(06)71389-X

[8] Gunn J., Zhang M.: Polyblend nanofibers for biomedical applications: Perspectives and challenges. Trends in Biotechnology, **28**, 189–197 (2010). https://doi.org/10.1016/j.tibtech.2009.12.006

[9] Cui W., Cheng L., Li H., Zhou Y., Zhang Y., Chang J.: Preparation of hydrophilic poly(L-lactide) electrospun fibrous scaffolds modified with chitosan for enhanced cell biocompatibility. Polymer, **53**, 2298–2305 (2012). https://doi.org/10.1016/j.polymer.2012.03.039

[10] Blackwood K. A., McKean R., Canton I., Freeman C. O., Franklin K. L., Cole D., Brook I., Farthing P., Rimmer S., Haycock J. W., Ryan A. J., MacNeil S.: Development of biodegradable electrospun scaffolds for dermal replacement. Biomaterials, **29**, 3091–3104 (2008). https://doi.org/10.1016/j.biomaterials.2008.03.037

[11] Lowery J. L., Datta N., Rutledge G. C.: Effect of fiber diameter, pore size and seeding method on growth of human dermal fibroblasts in electrospun poly(ε-caprolactone) fibrous mats. Biomaterials, **31**, 491–504 (2010). https://doi.org/10.1016/j.biomaterials.2009.09.072

[12] Kanimozhi K., Khaleel Basha S., Sugantha Kumari V.: Processing and characterization of chitosan/PVA and methylcellulose porous scaffolds for tissue engineering. Materials Science and Engineering: C, **61**, 484–491 (2016). https://doi.org/10.1016/j.msec.2015.12.084

[13] Bai S., Han H., Huang X., Xu W., Kaplan D. L., Zhu H., Lu Q.: Silk scaffolds with tunable mechanical capability for cell differentiation. Acta Biomaterialia, **20**, 22–31 (2015). https://doi.org/10.1016/j.actbio.2015.04.004

[14] Kim H. H., Song D. W., Kim M. J., Ryu S. J., Um I. C., Ki C. S., Park Y. H.: Effect of silk fibroin molecular weight on physical property of silk hydrogel. Polymer, **90**, 26–33 (2016). https://doi.org/10.1016/j.polymer.2016.02.054

[15] Huang Y., Onyeri S., Siewe M., Moshfeghian A., Madihally S. V.: *in vitro* characterization of chitosan–gelatin scaffolds for tissue engineering. Biomaterials, **26**, 7616–7627 (2005). https://doi.org/10.1016/j.biomaterials.2005.05.036

[16] Mao J. S., Zhao L. G., Yin Y. J., Yao K. D.: Structure and properties of bilayer chitosan–gelatin scaffolds. Biomaterials, **24**, 1067–1074 (2003). https://doi.org/10.1016/S0142-9612(02)00442-8

[17] Han D., Gouma P-I.: Electrospun bioscaffolds that mimic the topology of extracellular matrix. Nanomedicine: Nanotechnology, Biology and Medicine, **2**, 37–41 (2006). https://doi.org/10.1016/j.nano.2006.01.002

[18] Ravichandran R., Venugopal J. R., Sundarrajan S., Mukherjee S., Sridhar R., Ramakrishna S.: Composite poly-L-lactic acid/poly-(α,β)-DL-aspartic acid/collagen nanofibrous scaffolds for dermal tissue regeneration. Materials Science and Engineering: C, **32**, 1443–1451 (2012). https://doi.org/10.1016/j.msec.2012.04.024

[19] Tseng H-J., Tsou T-L., Wang H-J., Hsu S-H.: Characterization of chitosan–gelatin scaffolds for dermal tissue engineering. Journal of Tissue Engineering and Regenerative Medicine, **7**, 20–31 (2013). https://doi.org/10.1002/term.492

[20] Mandal B. B., Priya A. S., Kundu S. C.: Novel silk sericin/gelatin 3-D scaffolds and 2-D films: Fabrication and characterization for potential tissue engineering applications. Acta Biomaterialia, **5**, 3007–3020 (2009). https://doi.org/10.1016/j.actbio.2009.03.026

[21] Bhowmick S., Scharnweber D., Koul V.: *Co*-cultivation of keratinocyte-human mesenchymal stem cell (hMSC) on sericin loaded electrospun nanofibrous composite scaffold (cationic gelatin/hyaluronan/chondroitin sulfate) stimulates epithelial differentiation in hMSCs: *in vitro* study. Biomaterials, **88**, 83–96 (2016). https://doi.org/10.1016/j.biomaterials.2016.02.034

[22] Yukseloglu S. M., Sokmen N., Canoglu S.: Biomaterial applications of silk fibroin electrospun nanofibres. Microelectronic Engineering, **146**, 43–47 (2015). https://doi.org/10.1016/j.mee.2015.04.008

[23] Shi L., Yang N., Zhang H., Chen L., Tao L., Wei Y., Liu H., Luo Y.: A novel poly(γ-glutamic acid)/silk-sericin hydrogel for wound dressing: Synthesis, characterization and biological evaluation. Materials Science and Engineering: C, **48**, 533–540 (2015). https://doi.org/10.1016/j.msec.2014.12.047

[24] Ng K. W., Khor H. L., Hutmacher D. W.: *In vitro* characterization of natural and synthetic dermal matrices cultured with human dermal fibroblasts. Biomaterials, **25**, 2807–2818 (2004). https://doi.org/10.1016/j.biomaterials.2003.09.058

[25] Okamoto M., John B.: Synthetic biopolymer nanocomposites for tissue engineering scaffolds. Progress in Polymer Science, **38**, 1487–1503 (2013). https://doi.org/10.1016/j.progpolymsci.2013.06.001

[26] Cui W., Zhu X., Yang Y., Li X., Jin Y.: Evaluation of electrospun fibrous scaffolds of poly(DL-lactide) and poly(ethylene glycol) for skin tissue engineering. Materials Science and Engineering: C, **29**, 869–876 (2009). https://doi.org/10.1016/j.msec.2009.02.013

[27] Yooyod M., Ross G. M., Limpeanchob N., Suphrom N., Mahasaranon S., Ross S.: Investigation of silk sericin conformational structure for fabrication into porous scaffolds with poly(vinyl alcohol) for skin tissue reconstruction. European Polymer Journal, **81**, 43–52 (2016). https://doi.org/10.1016/j.eurpolymj.2016.05.023

[28] Wang Y. J., Zhag Y. Q.: Three-layered sericins around the silk fibroin fiber from *Bombyx mori* cocoon and their amino acid composition. Advanced Materials Research, **175–176**, 158–163 (2011). https://doi.org/10.4028/www.scientific.net/AMR.175-176.158

[29] Zhang Y-Q.: Applications of natural silk protein sericin in biomaterials. Biotechnology Advances, **20**, 91–100 (2002). https://doi.org/10.1016/S0734-9750(02)00003-4

[30] Brown B. N., Badylak S. F.: Expanded applications, shifting paradigms and an improved understanding of host–biomaterial interactions. Acta Biomaterialia, **9**, 4948–4955 (2013). https://doi.org/10.1016/j.actbio.2012.10.025

[31] Lamboni L., Gauthier M., Yang G., Wang Q.: Silk sericin: A versatile material for tissue engineering and drug delivery. Biotechnology Advances, **33**, 1855–1867 (2015). https://doi.org/10.1016/j.biotechadv.2015.10.014

[32] Lungu A., Albu M. G., Stancu I. C., Florea N. M., Vasile E., Iovu H.: Superporous collagen-sericin scaffolds. Journal of Applied Polymer Science, **127**, 2269–2279 (2013). https://doi.org/10.1002/app.37934

[33] Zhang H. P., Wang X. Y., Min S. J., Mandal M., Yang M. Y., Zhu L. J.: Hydroxyapatite/sericin composite film prepared through mineralization of flexible ethanol-treated sericin film with simulated body fluids. Ceramics International, Part A, **40**, 985–991 (2014). https://doi.org/10.1016/j.ceramint.2013.06.095

[34] McManus M. C., Boland E. D., Simpson D. G., Barnes C. P., Bowlin G. L.: Electrospun fibrinogen: Feasibility as a tissue engineering scaffold in a rat cell culture model. Journal of Biomedical Materials Research: Part A, **81**, 299–309 (2007). https://doi.org/10.1002/jbm.a.30989

[35] Vepari C., Kaplan D. L.: Silk as a biomaterial. Progress in Polymer Science, **32**, 991–1007 (2007). https://doi.org/10.1016%2Fj.progpolymsci.2007.05.013

[36] Altman G. H., Diaz F., Jakuba C., Calabro T., Horan R. L., Chen J., Lu H., Richmond J., Kaplan D. L.: Silk-based biomaterials. Biomaterials, **24**, 401–416 (2003). https://doi.org/10.1016/S0142-9612(02)00353-8

[37] Siritienthong T., Ratanavaraporn J., Aramwit P.: Development of ethyl alcohol-precipitated silk sericin/polyvinyl alcohol scaffolds for accelerated healing of full-thickness wounds. International Journal of Pharmaceutics, **439**, 175–186 (2012). https://doi.org/10.1016/j.ijpharm.2012.09.043

[38] Vulpe R., Popa M., Picton L., Balan V., Dulong V., Butnaru M., Verestiuc L.: Crosslinked hydrogels based on biological macromolecules with potential use in skin tissue engineering. International Journal of Biological Macromolecules, **84**, 174–181 (2016). https://doi.org/10.1016/j.ijbiomac.2015.12.019

[39] Vulpe R., Le Cerf D., Dulong V., Popa M., Peptu C., Verestiuc L., Picton L.: Rheological study of in-situ crosslinkable hydrogels based on hyaluronanic acid, collagen and sericin. Materials Science and Engineering: C, **69**, 388–397 (2016). https://doi.org/10.1016/j.msec.2016.07.003

[40] Kundu B., Kundu S. C.: Silk sericin/polyacrylamide *in situ* forming hydrogels for dermal reconstruction. Biomaterials, **33**, 7456–7467 (2012). https://doi.org/10.1016/j.biomaterials.2012.06.091

[41] Cao T-T., Zhang Y-Q.: Processing and characterization of silk sericin from *Bombyx mori* and its application in biomaterials and biomedicines. Materials Science and Engineering: C, **61**, 940–952 (2016). https://doi.org/10.1016/j.msec.2015.12.082

[42] Huang L., Tao K., Liu J., Qi C., Xu L., Chang P., Gao J., Shuai X., Wang G., Wang Z., Wang L.: Design and fabrication of multifunctional sericin nanoparticles for tumor targeting and pH-responsive subcellular delivery of cancer chemotherapy drugs. ACS Applied Materials and Interfaces, **8**, 6577–6585 (2016). https://doi.org/10.1021/acsami.5b11617